ELSEVIER

Ceramics International 33 (2007) 803–810

CERAMICS INTERNATIONAL

www.elsevier.com/locate/ceramint

A novel approach for magnesia hydration assessment in refractory castables

Rafael Salomão [a], L.R.M. Bittencourt [b], V.C. Pandolfelli [a,*]

[a] *Materials Engineering Department, Federal University of São Carlos, Rod. Washington Luíz, km 235 São Carlos, SP, Brazil*
[b] *Magnesita S.A., Praça Louis Ensch, 240 Contagem, MG, Brazil*

Received 7 November 2005; received in revised form 5 December 2005; accepted 24 January 2006
Available online 18 April 2006

Abstract

Magnesium oxide (MgO) or magnesia is one of the most important raw materials in the refractory industry. Because of its high refractoriness (melting point of 2800 °C) and corrosion resistance, the presence of this oxide in refractory compositions promotes an increase in the performance of pre-shaped linings for steel production [C.M. Peret, J.A. Gregolin, L.I.L Faria, V.C. Pandolfelli, Patent generation and the technological development of refractories and steelmaking, Refract. Appl. News, submitted for publication; M. Rigaud, Z. Ningsheng, Major trends in refractories industry at the beginning of the 21st century, China's Refract. 11 (2) (2002) 3–8; W.E. Lee, R.E. Moore, Evolution of in-situ refractories in the 20th century, J. Am. Ceram. Soc. 81 (6) (1998) 1385–1410; A. Nishikawa, Technology of monolithic refractories, Tokyo: Technical report No. 33-7, PLIBRICO Japan Co. Ltd, 1984, pp. 98–101]. Nevertheless, in refractory castables formulations, magnesia additions are restricted to coarse particles (usually above 50 μm) and contents of up to 10 wt.% due to their high tendency to react with water and the following great volumetric expansion promoted by this reaction [G.K. Layden, G.W. Brindley, Kinetics of vapor-phase hydration of magnesium oxide, J. Am. Ceram. Soc. 46 (11) (1963) 518–522; A. Kitamura, K. Onizuka, K. Tanaka, Hydration characteristics of magnesia, Taikabutsu Overseas 16 (3) (1995) 3–11; A. Yoschida, T. Nemoto, A. Kaneyasu, Evaluation method for hydration resistance of magnesia fine powder and effect of B_2O_3 content in magnesia raw materials, in: Proceedings of UNITECR' 2003, 2003, pp. 21–30; R.A. Wogelius, K. Refson, D.G. Fraser, G.W. Grime, J.P. Goff, Periclase surface hydroxylation during dissolution, Geochim. Cosmochim. Acta 59 (9) (1995) 1875–1881; A. Kaneyasu, S. Yamamoto, A, Yoshida, Magnesia raw materials with improved hydration resistance, Taikabutsu Overseas 17 (2) (1996) 21–26; P. Brandão, G.E. Gonçalves, A.K. Duarte, Mechanisms of hydration/carbonation of basic refractories—Part I, Refract. Appl. News 3(2) (1998) 6–9; P. Brandão, G.E. Gonçalves, A.K. Duarte, Mechanisms of hydration/carbonation of basic refractories—Part II: investigation of the kinetics of formation of brucite in fired basic bricks, Refract. Appl. News 3 (2) (1998) 9–11; P. Brandão, G.E. Gonçalves, A.K. Duarte, Mechanisms of hydration/carbonation of basic refractories—Part III, Refract. Appl. News 8 (6) (1998) 23–26; S. Chatterji, Mechanism of expansion of concrete due to the presence of dead-burnt CaO and MgO, Cem. Concr. Res. 25 (1) (1995) 51–56]. Despite the great number of studies describing the behavior of powdered magnesia or high-magnesia bricks, not much research has systematically been done related to its hydration behavior in castables [A. Yoschida, T. Nemoto, A. Kaneyasu, Evaluation method for hydration resistance of magnesia fine powder and effect of B_2O_3 content in magnesia raw materials, in: Proceedings of UNITECR' 2003, 2003, pp. 21–30; S. Chatterji, Mechanism of expansion of concrete due to the presence of dead-burnt CaO and MgO, Cem. Concr. Res. 25 (1) (1995) 51–56; T.A. Bier, C. Parr, C. Revais, H. Fryda, Chemical interactions in calcium aluminate cement based castables containing magnesia, in: Proceedings of UNITECR' 1997, 1997, pp. 15–21; D. Jeong, H. Kim, Y. Kim, S. Lee, Development and application of basic dam block for Tundish, J. Tech. Assoc. Refract. Japan 23 (1) (2003) 4–10; K.G. Ahari, J.H. Sharp, W.E. Lee, Hydration of refractory oxides in castable bond systems—I: alumina, magnesia and alumina–magnesia mixtures, J. Eur. Ceram. Soc. 22 (2002) 495–503; K.G. Ahari, J.H. Sharp, W.E. Lee, Hydration of refractory oxides in castable bond systems—II: alumina–silica and magnesia–silica mixtures, J. Eur. Ceram. Soc. 23 (2003) 3071–3077; Y. Koga, M. Sato, K. Sekeguchi, S. Iwamoto, Effects of alumina cement grade and additives on alumina–magnesia castable containing aluminum lactate, Taikabutsu Overseas 18 (1) (1997) 43–47]. In this paper, aspects of magnesia hydration were briefly reviewed. Novel insights concerning magnesia hydration products generated under different curing conditions were attained adapting techniques already used in castables study.

Keywords: Magnesia hydration; Refractory castables; Curing temperature

* Corresponding author. Tel.: +55 16 260 8252; fax: +55 16 260 8252.
E-mail addresses: vicpando@power.ufscar.br, pers@iris.ufscar.br (V.C. Pandolfelli).

0272-8842/$32.00
doi:10.1016/j.ceramint.2006.01.004

1. Introduction

1.1. Magnesia hydration/dehydration mechanisms

The hydration of magnesia is carried out by the contact of this oxide with liquid water (as in the mixing and curing steps of castables), water vapor (during the drying process) or moisture (during the storage period). The hydration products formed are described in the literature as follows [5–12]

$$MgO + H_2O \rightarrow Mg(OH)_2 \quad (1)$$

$$MgO + H_2O + CO_2 \rightarrow MgO + H_2CO_3 \rightarrow MgCO_3 \quad (2)$$

The magnesium hydroxide or brucite, resulting from Eq. (1), is crystalline and it is formed when there is a great availability of water, as in castable structures. The brucite formation promotes a significant increase in the pH allowing CO_2 to be dissolved in water and the generation of carbonic acid (H_2CO_3). This acid reacts with magnesium oxide (MgO) resulting in magnesium carbonate or magnesite, as pointed out in Eq. (2). Magnesite can also be formed during the storage of magnesia sinters and pre-shaped parts and presents a mould aspect.

Both hydration routes present a similar effect: a remarkable 2.5-fold volumetric expansion [5–8]. Nevertheless, as magnesite is preferably formed on the surface of the exposed MgO, brucite is normally associated to the volumetric variation and its effects on the refractory structures and properties. Its generation and the consequent volumetric expansion can be described by two routes: single crystals or polycrystalline MgO hydration.

1.2. Hydration of magnesia single crystals

The single crystals of magnesia used in many research studies to understand the hydration mechanism are usually obtained by fusion on a laboratorial scale and under controlled conditions of dead burnt MgO sinter [5,6,8]. In practice, however, the magnesia grains used as refractory raw materials are polycrystalline and could generally be described as several single crystals bonded together.

When an MgO single crystal surface is exposed to water, the magnesia cubic structure is changed to brucite's hexagonal one or to the rhombohedral when magnesite is formed. The volumetric expansion produces a striped micro-cracked pattern, as a result of the hexagonal structure morphology. In the early stages, the hydration rate is slow and strongly dependent on the reaction surface. This step is known as the induction period and is shown in Fig. 1(a) [6].

After this step, hydration continues towards the center of the crystal. The micro-cracks which have been produced also help to ease the diffusion of water increasing the hydration rate. After the formation of a brucite layer, the process becomes water diffusion controlled and the hydration rate is decreased to lower rates. Reports in the literature pointed out the completion of single crystal hydration after some weeks of water exposure [6].

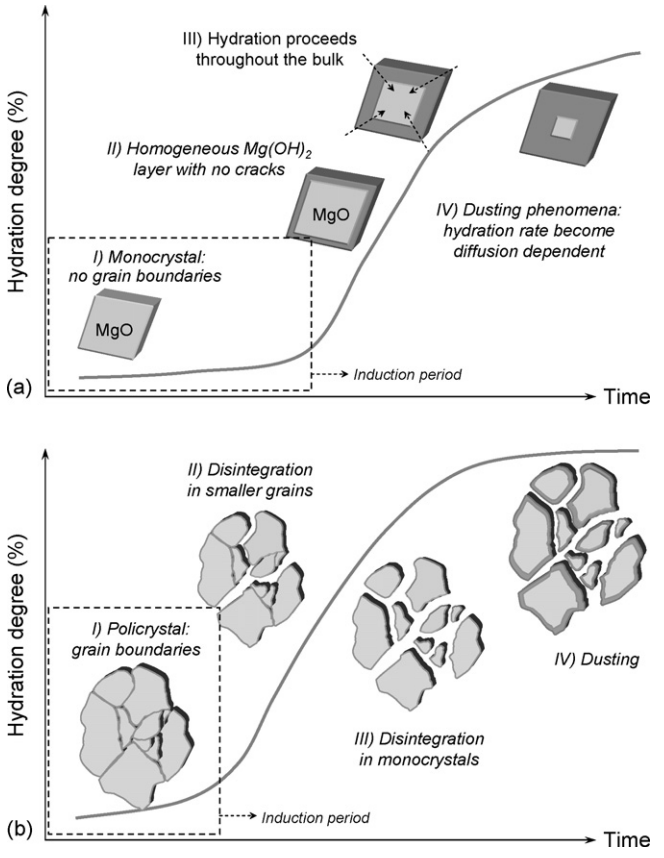

Fig. 1. Hydration mechanisms of: (a) magnesia monocrystal and (b) of polycrystalline magnesia [6,10–12].

1.3. Hydration of polycrystalline magnesia

The magnesia particles used in refractories, such as sinters and fused aggregates, are polycrystalline structures, which are characterized by grains of different crystallographic orientation and clearly defined interfaces (grain boundaries). When compared with the center of the grain, the boundaries present regions with higher free energy which are more likely to react with water [6–8]. As soon as a thin brucite layer is formed on the surface of a single crystal, the following volumetric expansion presents only a small or no effect on the bulk of the particle. In a polycrystalline particle, the volumetric expansion is firstly carried out at the grain boundary with no or small room for expansion accommodation.

In these early hydration stages, the magnesia expansion can be indirectly detected by the increase in the elastic modulus of the refractory and a reduction in porosity [24]. In both cases, it is associated to the filling of the porosity with brucite. However, as hydration proceeds, the tensions brought about become strong enough to break the boundary bonds, breaking apart the original particle into several other smaller ones. As a consequence, the porosity, the total surface area and the hydration rate of the material are drastically enlarged and, in parallel, the rigidity is reduced and the induction period becomes shorter than that observed for single crystals (Fig. 1(b)). This process continues up to the total hydration

of the grain boundaries and, after this point, the hydration proceeds as described for single crystals [6].

The hydrate layer usually behaves as a barrier for later hydration and volumetric expansion. If this pre-formation of the brucite and carbonate layers occurs before the conformation of the particles, the damages caused by the volumetric expansion are reduced [10–12]. This aspect is currently used by the refractory manufactures in order to prevent the effects of hydration in magnesia pre-shaped products. The best outcome of this technique is attained by storing the dead burnt material for several weeks in a ventilated environment before using.

Another important consequence of brucite generation is the resulting structure after thermal treatment [19–23]. Brucite starts to be thermally decomposed at 350–375 °C and above 600 °C no further thermal decomposition is observed. Therefore, if a partially hydrated material is heated between 500 °C and 800–950 °C, the brucite hexagonal structure tends to be converted into a cubic magnesia one. Because, at this temperature range, the total conversion is not fully carried out, the final structure is a porous, high surface area, micro-cracked one due to the volumetric reduction experienced. On the other hand, if the thermal treatment of partially hydrated magnesia were carried out above 950 °C, the crystals start growing, followed by the surface area reduction. Above 1200 °C, sintering begins and the magnesia cubic structure is restored.

1.4. Qualitative and quantitative techniques employed in the study of magnesia hydration

Hydration of magnesia has been studied since the first decades of the 20th century, due to its large applications in agriculture and medicine, such as soil modifiers and anti-acid compounds, respectively [5]. For refractory applications, on the other hand, research is more recent and focused on practical aspects: quantification and identification of hydration products and the reduction of expansion effects on the refractory products.

One of the most common experiments found in the literature is the hydration test. It consists of exposing a known amount of magnesia to a water source (liquid, vapor or both) [6–9]. Based on the samples' weight variation before and after the exposure and on the stoichiometric molecular weight difference between magnesia and brucite, the degree of hydration and the reaction rate, can be calculated for a certain temperature as stated in Eq. (3):

$$\alpha = \left(\frac{\Delta m}{m_{\mathrm{l}}}\right) \times \left(\frac{1}{44.7}\right) \tag{3}$$

where, α is the hydration degree (varying from 0% up to 100%); Δm the mass variation during the reaction and the (1/44.7) term is the theoretical value of α, if the reaction is fully carried out.

The tests indicated that the degree of hydration can be drastically influenced by the environmental conditions. A temperature range varying from 73 °C up to 200 °C with different time exposure periods (0.5 h up to several months) can generate consistent time–temperature hydration maps. These maps point out that the hydration rate increases exponentially with the temperature above 90–100 °C. Other important contribution of these tests is related to the expansion effect for MgO compositions presenting different hydration rates. Considering, for example, 135 °C and 150 °C, both temperatures led to the same hydration degree ($\alpha = 0.9$), but at a different time exposure (70 h and 15 h, respectively), which resulted in distinct damages. At 135 °C, because of the lower hydration rate, the surrounding structure can partially absorb the volumetric expansion. At 150 °C, the faster rate generates a more localized tension, resulting in a more intense cracking process [24].

When the temperature is above 100 °C, the use of an autoclave is required in order to prevent water ebullition. The systems described in the literature vary from a simple close vessel, to a more sophisticated apparatus with very accurate temperature and pressure controls [6–9]. The hydration tests carried out in autoclaves present, as their major advantage, shorter times of exposure and a more severe testing condition. The most employed hydration experiment consists of exposing a sample in an autoclave at 152 °C, for 3 h, in a saturated water vapor atmosphere. In order to correctly perform the test, there must be liquid water inside the vessel, but it should not touch the sample [6].

After hydration tests conducted in autoclave or other conditions, the MgO hydration products formed are identified and quantified. The X-ray diffraction (XRD) analysis pointed out brucite as being mainly responsible for the volumetric expansion of magnesia [8]. Afterwards, the X-ray peak intensities under different hydration conditions can quantify the progress of brucite evolution and its crystal sizes. In addition, the infrared spectroscopy (IRS) can access the low crystallinity hydration products, such as magnesite [10–12]. Thermogravimetry (TG) and differential scanning calorimetry (DSC) were also used in order to identify the thermal reactions involved in the magnesia/brucite/magnesite system, mainly during the decomposition of the hydration products [9]. These results allowed a better understanding of the calcining conditions for magnesia production. Finally, the hydration progress was also followed by ultrasonic measurements of the elastic modulus (MOE) [24]. This technique pointed out that, at the beginning of hydration, the rigidity of the refractory may increase as the result of pores filling and, at the final stages, it falls drastically, because of the volumetric expansion and cracking.

Despite progress in the understanding of the magnesia hydration mechanism obtained using these techniques, few contributions were directed to its role in castable formulations. This can be attributed to the inherent complexity of the system, to the difficulty imposed by the usual characterization techniques to deal with castable samples (usually, the size of the sample required for analytical methods is smaller than the coarse particles used in the formulation) and to the technological aspects involved in the publication of the research results.

In this paper, the hot air permeametry (HAP) [25,26], the mechanical strength evaluated under diametrical compression and the thermogravimetry of castable samples [27–29] were employed to study magnesia containing castable samples. These techniques were recently explored in the literature as powerful tools to investigate the drying behavior of refractory castables and the effects of drying additives, such as polypropylene fibers [26,30].

2. Castable composition and preparation of samples

A vibrated high alumina refractory castable composition containing 6 wt.% of magnesia sinter (Magnesita S.A., Brazil), 6 wt.% of calcium aluminate cement (CA14M, Almatis, US), 5.5 wt.% of water and 0.2 wt.% of a sodium phosphate (Synth, Brazil) was used in the tests. A detailed description of the raw materials can be found in Table 1. The dry mixing and the water addition were carried out in a paddle mixer for 10 min.

After this time, the formulations were cast under vibration in cylindrical molds for hot air permeametry (70 mm diameter × 26 mm height); drying tests, porosity and mechanical strength measurements (40 mm × 40 mm) and apparent volumetric expansion (AVE) tests (70 mm × 70 mm). The curing time was performed in an acclimatized chamber Vöetch 2020, in an environment with humidity close to 100% and at different temperatures (8 °C, 30 °C, 50 °C and 80 °C) for 7 days.

Before testing, the samples used for porosity measurements were dried for 24 h in silica-gel, at the curing temperature, in order to remove moisture. Those used in the other techniques were tested just after the curing time.

3. Hot air permeametry

In the hot air permeametry technique, an airflow generated by a high-pressure pump is forced to percolate a castable sample placed in an electric furnace. This technique is especially suitable to detect temperature dependent permeability variations, with no need of previous thermal treatment [25,26]. For the magnesia containing castables, the use of such a technique enabled us to quantify the permeability changes in the first heat-up of the samples. Green and humid samples were placed in the equipment, under a pressure gradient of 0.3 MPa. Temperature was kept constant at 30 °C, 50 °C and 80 °C during 7 days. The flow rate values were computer recorded (1 data/min).

In Fig. 2(a), the first 24 h of the test presented a typical HAP profile [26]. As soon as the water is being released, the airflow rate starts increasing, reaching an almost constant level after 10 h. The higher the furnace temperature, the faster the air flow rate stabilization is and the higher the final airflow level. This is associated to the speed of the water removal and to the changes of hydrated phases of calcium aluminate cement.

After the samples were partially dried (24 h), no changes in the airflow rate are expected unless other structural rearrangements in the porous media is verified, as shown for the sample kept at 30 °C for 7 days (Fig. 2(b)). For those heated at 50 °C and 80 °C, however, after 72 h and 36 h, respectively, the airflow rate started to increase, reaching the upper limit of the flow meter used. The visual inspection of these two samples has shown the presence of cracks and volumetric expansion, whereas the sample kept at 30 °C remained intact.

As these cracks were not observed in alumina based magnesia-free castables tested in similar conditions [25,26], they can be attributed to the formation of magnesium hydroxide and magnesium carbonate. No permeability reduction was observed either in the initial stages of drying, or during the magnesia hydration reaction. These results suggested that, differently to what was reported in the literature [15,31], during the drying of these materials, explosive spalling is more likely to occur due to the weakening caused by the crack formation than due to permeability reductions.

Table 1
Refractory castable formulation studied

Raw materials	wt.%
Matrix ($D_{Particle} < 100$ μm	
Calcined aluminas[a]	3
Calcium aluminate cement (CA14M)[a]	6
Magnesia sinter[b]	6
Aggregates ($D_{Particle} \geq 100$ μm, $D_{Max} = 5.6$ mm)	
White electrofused alumina[c]	85
Dispersant agent	
Sodium phosphate[d]	0.2

[a] Almatis (US).
[b] Magnesita S.A. (Brazil).
[c] Elfusa (Brazil).
[d] Synth (Brazil).

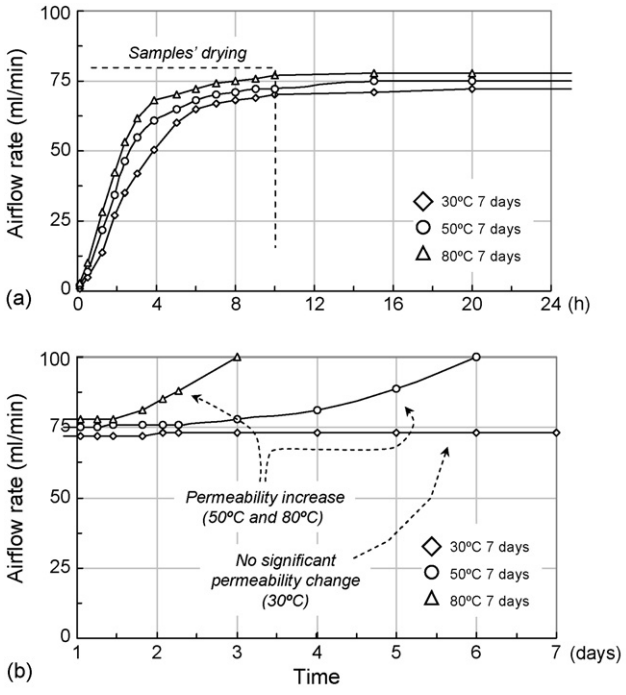

Fig. 2. Hot air permeametry for magnesia containing castables: (a) first 24 h and (b) after 7 days at constant temperatures.

4. Mechanical strength, porosity measurements and volumetric expansion test

The expansion that follows the hydration of the MgO can reach up to 2.5 times its initial volume (real volumetric expansion). Nevertheless, in castable formulations, the expansion observed is frequently smaller (apparent volumetric expansion) due to three main effects: (1) the presence of other raw materials that do not hydrate (as electrofused alumina, for example); (2) the use of a binder that can restrain the MgO volumetric expansion and (3) the expansion accommodation in the structure porosity [32]. Therefore, the concept of apparent volumetric expansion comes out as a quantitative measurement of the competition between these effects' that could increase or inhibit MgO containing product expansion.

Unlike the density measurement based methods (as helium picnometry) that assess all open volume inside the materials structure, the apparent volumetric expansion refers to the external volume of the castable. As traditional methods usually require small samples, the AVE measurements become a practical, fast, representative and efficient way to quantify the effects of MgO hydration in refractory castables.

The AVE observed in castables can be evaluated measuring the dimensions of the samples before and after being exposed to a certain hydration condition. However, the values obtained can be affected by the presence of the coarse aggregates that usually produce rough surfaces. In order to minimize this effect, thin wall molds, designed with a special non-adherent polymeric material, were used in this study. In these molds, the samples were free to expand without any significant restriction, allowing a uniform measurement of the samples' dimensions during their expansion.

The AVE test consists of measuring the dimensions of a 70 mm × 70 mm cylindrical sample under a certain hydration condition (in the present study, over 7 days in a humid saturated environment at different temperatures: 8 °C, 30 °C, 50 °C and 80 °C), as schematically shown in Fig. 3. The AVE is calculated considering the initial volume of the samples as a reference and can be described by the following equations:

$$V_i = \frac{H_i \times \pi \times (D_i - 2t)^2}{4} \tag{4}$$

$$\mathrm{AVE} = 100 \times \frac{V_\mathrm{E} - V_0}{V_0} \tag{5}$$

Eq. (4) is used to calculate the volume of cylindrical samples at a particular time, where V_i is the volume; H, the height; D, the diameter and t the mold wall thickness. For the AVE parameter; V_0 is the initial volume of the sample and V_E is the correspondent volume after hydration and expansion.

The splitting tensile strength was obtained according to the ASTM C496-96 standard in a MTS TestStar II equipment. A constant loading rate of 42 N/s (1000 kPa/min) was used. Five specimens for each testing condition were tested. The total porosity of the samples was measured by the immersion method, using kerosene as immersion fluid.

Fig. 4 shows the mechanical strength, total porosity and the apparent volumetric expansion of the castables cured in different temperatures over 7 days. Three distinct behaviors were observed. (1) Up to the seventh day, the mechanical strength attained for the 8 °C cured castable increased, porosity was reduced and no expansion was observed. (2) For those cured at 50 °C and 80 °C, the mechanical strength achieved its highest value at the lowest porosity. After this point, volumetric expansion was observed, followed by a drop in the mechanical strength and by a porosity increase. (3) The castables cured at 30 °C presented an intermediate behavior, with a mechanical strength reduction, a porosity increase and a volumetric expansion which were only observed after the sixth day.

Similar results were reported in the literature for magnesia bricks exposed to water vapor [24]. In that case, an increase in the modulus of elasticity (MOE) values and porosity reduction in the early stages of hydration was observed. This was followed by a reduction in MOE values and a porosity increase of up to more than 50%, due to cracking. This effect is related to the magnesia volumetric expansion. The authors also pointed out that at the first stages of hydration, only a small quantity of brucite was formed and the volume expansion was accom-

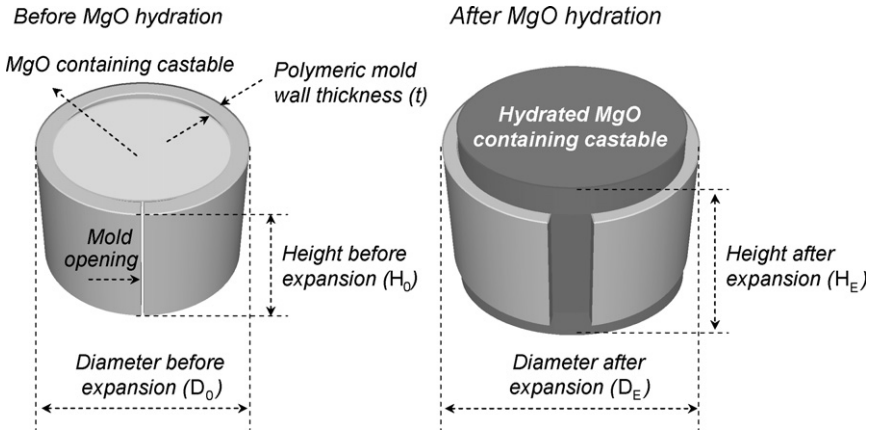

Fig. 3. Schematic view of the apparent volumetric expansion (AVE) test (the mold wall thickness was thinner that shown in this figure).

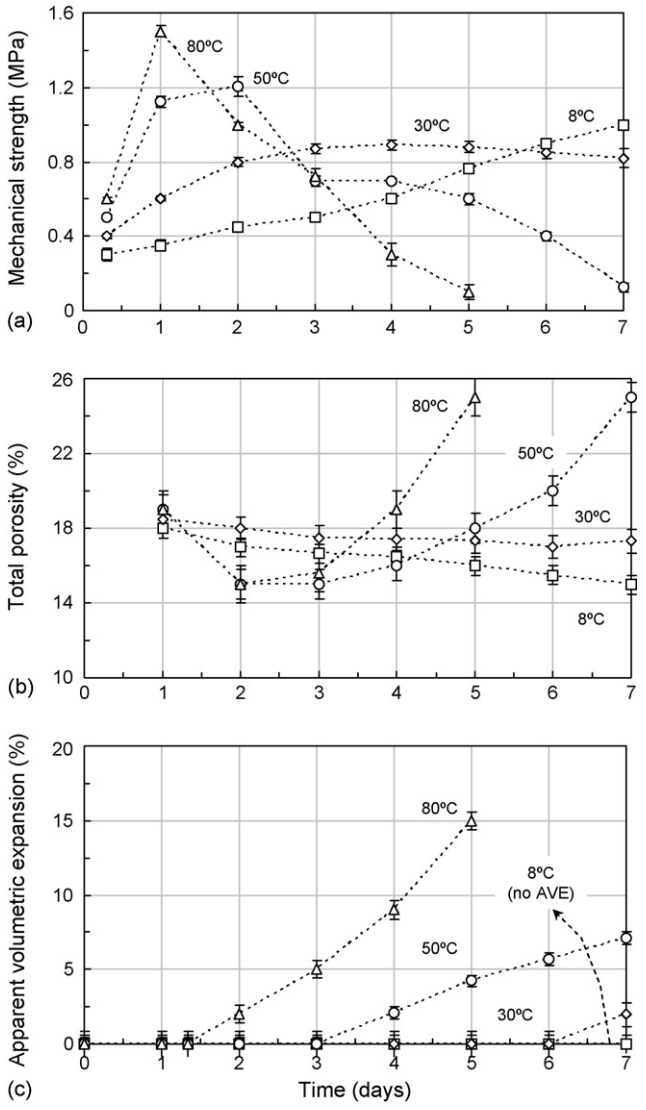

Fig. 4. (a) Splitting tensile strength; (b) total porosity measurements and (c) apparent volumetric expansion (AVE) test for magnesia containing castables under different hydration conditions.

modated by the sample's pores. The porosity filling increased the mechanical properties of the material as shown by the MOE [24] and the mechanical strength of the samples produced in the present study. However, after a certain reaction degree, there was no more room to accommodate the hydration products and compressive tensions were brought about. As they reached the mechanical strength of the material, the apparent volumetric expansion and crack formation were observed. This mechanism is schematically demonstrated in Fig. 5.

This process is strongly dependent on the hydration rate and temperature. The faster the brucite is generated, the quicker the porosity is filled and the tensions are developed. The results in Fig. 4 were in accordance with this statement. Samples cured at a higher temperature presented earlier and more significant problems related to magnesia hydration, whereas they were almost not observed at low curing temperatures (8 °C and 30 °C, respectively).

Another aspect to be considered is the curing temperature effect on cement hydration [33–35]. As for magnesia, the temperature strongly influences calcium aluminate cement hydration. Generally, higher curing temperatures accelerate the hydration rates leading to superior mechanical strength levels and greater porosity reduction. These effects cause opposite impacts in magnesia hydration: higher mechanical strength structures require further expansion to cause damage; on the other hand, the smaller porosity reduces the possibilities of brucite formation accommodation. The results attained suggest that the last hypothesis presented a more significant effect.

5. Drying tests

The drying tests were performed in a thermogravimetric apparatus developed by the authors' research group, which allows for simultaneous recording of the mass variations and temperature profile inside the furnace and at the sample's surface [27–29]. A heating rate of 10 °C/min was applied in the temperature range of 20–600 °C. The percentage of weight loss (W, %), representing the cumulative fraction of water released during the heat-up divided by the total amount of water initially

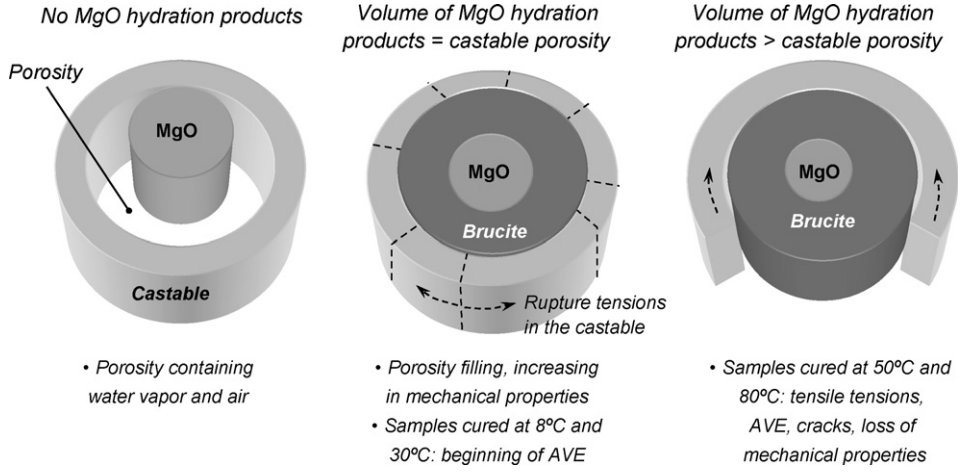

Fig. 5. Schematic view of the mechanical damage caused by the apparent volumetric expansion (AVE) during the magnesia hydration.

present in the body, and the drying rate (dW/dt), were evaluated based on the following equations:

$$W(\%) = 100 \times \frac{M_0 - M}{M_0 - M_F} \quad (6)$$

$$\left(\frac{dW}{dt}\right)_i = \frac{W_{i+10} - W_{i-10}}{t_{i+10} - t_{i-10}} \quad (7)$$

where M is the instantaneous mass recorded at time t_i during the heating stages; M_0 the initial mass and M_F is the final mass of the tested sample.

Tests were conducted: (1) in samples cured at 50 °C for up to 7 days (Fig. 6(a)) and (2) in samples cured at 8 °C, 30 °C, 50 °C and 80 °C for 7 days (Fig. 6(b)). The first condition reveals the kinetics of the magnesia hydration reaction and the second ones shows its dependence on the temperature at the same heating conditions. Fig. 6 also presents the results of a high-purity powdered $Mg(OH)_2$ samples tested.

The drying behavior of magnesia containing castables presented three complementary steps [27,30]. Evaporation, below 100 °C, which depends strongly on the environmental conditions (temperature and humidity) and usually presents a low drying rate. Secondly, above 100 °C, the mass loss through water ebullition which results in a higher drying rate because of the pressurization of the water vapor. At this stage, explosive spalling occurs if this pressure becomes greater than the mechanical strength of the castable. Thirdly, above 250 °C, where the hydration products (cement, aluminum hydroxide and brucite, in this case) decomposition starts and depending on the system, extending up to 600 °C or higher.

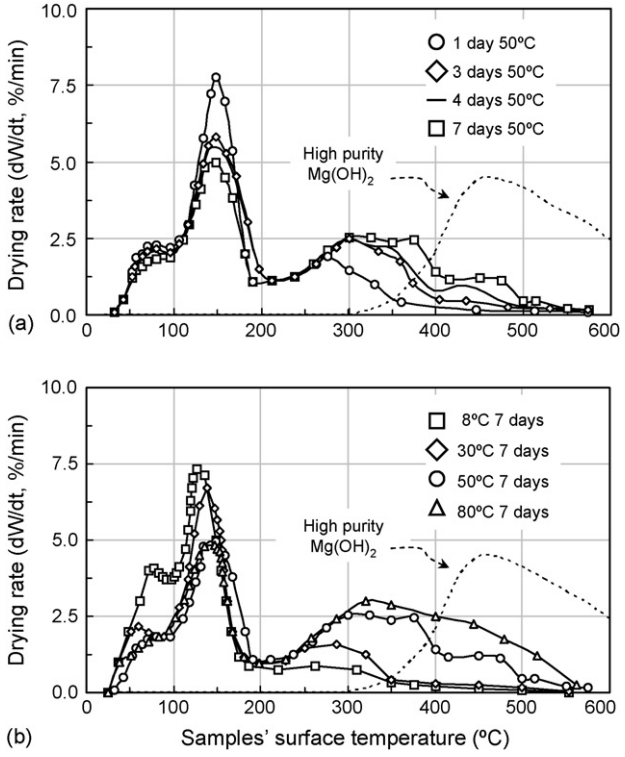

Fig. 6. Drying behavior of magnesia containing castables after different hydration conditions: (a) during 7 days at 50 °C and (b) after 7 days at different temperatures.

Fig. 6(a) shows the drying tests results carried out in samples cured at 50 °C for different periods. It can be pointed out that the amount of water released in each drying stage and the hydration products which were generated changed with the increase in the curing time. On the first day, an intense ebullition peak in the 100–200 °C range, followed by a well defined C_3AH_6 decomposition region [35] (200–350 °C) and no evidence of magnesia hydration (above 350 °C, as seen by the decomposition peak for the high-purity $Mg(OH)_2$ sample), were observed. This is an indication that cement and magnesia presented in the formulation are in their early stages of hydration, consuming a small part of the total water available. On the third day, the intensity of evaporation and ebullition peaks were reduced and the cement hydrates decomposition was enhanced. Up to this curing time, no indicative of magnesia hydration appeared. Between the third and the seventh day, a new hydrated phase, identified as magnesium hydroxide, started to decompose above 350 °C.

A similar effect is presented in Fig. 6(b), for the samples cured for 7 days at different temperatures. At lower temperatures (8 °C and 30 °C), the cement hydration level is reduced and no brucite was formed. As the curing temperature increased from 30 °C to 50 °C and 80 °C, differences in the dehydration peaks began to show up: cement hydration was highly increased (between 200 °C and 350 °C) and, simultaneously, a significant brucite dehydration peak could be observed. For the 80 °C cured samples, the cement and brucite dehydration peaks joint together, generating a single broad band.

The results of Fig. 6 can be related to those reported in Figs. 2 and 4. For the samples cured at 50 °C for 7 days, the first sign of magnesia hydration was simultaneous to the increase of the apparent volumetric expansion, porosity reduction and the loss of mechanical strength (fourth day). The same effect can be detected for the different curing temperature ones.

These results suggested that the level of mechanical damage caused is related to the amount of brucite formed and the rate that it occurred. At low curing temperatures (below 50 °C for the present system), a small quantity of brucite is slowly formed. Therefore, the volumetric expansion can be easily accommodated in the available porosity and low tension levels are developed. If the curing temperature increases, more brucite is formed in a short period of time. Consequently, the expansion accommodation becomes difficult and the structure is tensioned and cracked. In general, the increase in the curing time makes this effect worst, as a greater amount of brucite is produced and higher mechanical damage is caused.

6. Final remarks

This novel approach proposed to evaluate magnesia hydration in refractory castables has brought some new insights to its behavior in these materials. The hot air permeametry technique showed that no permeability reduction is expected during the drying of the magnesia containing

castables. Indeed, the likelihood of permeability increase is high because of the cracks generated in the curing time. The simultaneous evaluation of mechanical strength, apparent volumetric expansion and dehydration profile showed that the amount of brucite produced is simultaneously dependent on the time and temperature at which the samples were exposed. If the temperature is in the range of 20–30 °C, a longer time is required to initiate the reaction and to accommodate brucite formation into the castable porosity. The results also support that, at a low temperature (8 °C), the reaction driving force is so small that practically no brucite is formed up to 7 days of testing. On the other hand, if higher temperatures are used (50 °C and 80 °C), hydration starts earlier and reaches a higher reaction rate and intensity. Considering a same curing temperature, the longer the exposure to the hydration condition is, the higher the reaction degree attained. Depending on the temperature used, for the same time period, the final hydration level can be low (8 °C and 30 °C) or high (50 °C and 80 °C), with different consequences for castable properties.

Acknowledgments

The authors are thankful to the Brazilian Research Founding FAPESP, Alcoa Alumínio (Brazil) and Magnesita S.A. (Brazil) for supporting this work.

References

[1] C.M. Peret, J.A. Gregolin, L.I.L Faria, V.C. Pandolfelli, Patent generation and the technological development of refractories and steelmaking, Refract. Appl. News, submitted for publication.
[2] M. Rigaud, Z. Ningsheng, Major trends in refractories industry at the beginning of the 21st century, China's Refract. 11 (2) (2002) 3–8.
[3] W.E. Lee, R.E. Moore, Evolution of in-situ refractories in the 20th century, J. Am. Ceram. Soc. 81 (6) (1998) 1385–1410.
[4] A. Nishikawa, Technology of monolithic refractories, Tokyo: Technical report No. 33-7, PLIBRICO Japan Co. Ltd, 1984, pp. 98–101.
[5] G.K. Layden, G.W. Brindley, Kinetics of vapor-phase hydration of magnesium oxide, J. Am. Ceram. Soc. 46 (11) (1963) 518–522.
[6] A. Kitamura, K. Onizuka, K. Tanaka, Hydration characteristics of magnesia, Taikabutsu Overseas 16 (3) (1995) 3–11.
[7] A. Yoschida, T. Nemoto, A. Kaneyasu, Evaluation method for hydration resistance of magnesia fine powder and effect of B_2O_3 content in magnesia raw materials, in: Proceedings of UNITECR' 2003, 2003, pp. 21–30.
[8] R.A. Wogelius, K. Refson, D.G. Fraser, G.W. Grime, J.P. Goff, Periclase surface hydroxylation during dissolution, Geochim. Cosmochim. Acta 59 (9) (1995) 1875–1881.
[9] A. Kaneyasu, S. Yamamoto, A. Yoshida, Magnesia raw materials with improved hydration resistance, Taikabutsu Overseas 17 (2) (1996) 21–26.
[10] P. Brandão, G.E. Gonçalves, A.K. Duarte, Mechanisms of hydration/carbonation of basic refractories—Part I, Refract. Appl. News 3 (2) (1998) 6–9.
[11] P. Brandão, G.E. Gonçalves, A.K. Duarte, Mechanisms of hydration/carbonation of basic refractories—Part II: investigation of the kinetics of formation of brucite in fired basic bricks, Refract. Appl. News 3 (2) (1998) 9–11.
[12] P. Brandão, G.E. Gonçalves, A.K. Duarte, Mechanisms of hydration/carbonation of basic refractories—Part III, Refract. Appl. News 8 (6) (1998) 23–26.
[13] S. Chatterji, Mechanism of expansion of concrete due to the presence of dead-burnt CaO and MgO, Cem. Concr. Res. 25 (1) (1995) 51–56.
[14] T.A. Bier, C. Parr, C. Revais, H. Fryda, Chemical interactions in calcium aluminate cement based castables containing magnesia, in: Proceedings of UNITECR' 1997, 1997, pp. 15–21.
[15] D. Jeong, H. Kim, Y. Kim, S. Lee, Development and application of basic dam block for Tundish, J. Tech. Assoc. Refract. Japan 23 (1) (2003) 4–10.
[16] K.G. Ahari, J.H. Sharp, W.E. Lee, Hydration of refractory oxides in castable bond systems—I: alumina, magnesia and alumina–magnesia mixtures, J. Eur. Ceram. Soc. 22 (2002) 495–503.
[17] K.G. Ahari, J.H. Sharp, W.E. Lee, Hydration of refractory oxides in castable bond systems—II: alumina–silica and magnesia–silica mixtures, J. Eur. Ceram. Soc. 23 (2003) 3071–3077.
[18] Y. Koga, M. Sato, K. Sekeguchi, S. Iwamoto, Effects of alumina cement grade and additives on alumina–magnesia castable containing aluminum lactate, Taikabutsu Overseas 18 (1) (1997) 43–47.
[19] R. Gordon, W.D. Kingery, Thermal decomposition of brucite: electron and optical microscope studies, J. Am. Ceram. Soc. 49 (12) (1966) 654–660.
[20] M.G. Kim, U. Dhamen, A.W. Searcy, Structural transformation in the decomposition of $Mg(OH)_2$ and $MgCO_3$, J. Am. Ceram. Soc. 70 (3) (1987) 146–154.
[21] M.G. Kim, U. Dahmen, A.W. Searcy, Shape and size of crystalline MgO particles formed by the decomposition of $Mg(OH)_2$, J. Am. Ceram. Soc. 71 (8) (1988) C-373–C-375.
[22] H. Kim, J. Kang, M.Y. Song, S.H. Park, D.G. Park, H. Kweon, S.S. Nam, Surface modification of MgO micro-crystals by cycles of hydration-dehydration, Bull. Korean Chem. Soc. 20 (7) (1999) 786–790.
[23] V.S.S. Birchal, S.D.F. Rocha, V.S.T. Ciminelli, The effect of magnesite calcination conditions on magnesia hydration, Miner. Eng. 13 (14) (2000) 1629–1633.
[24] P. Lauzon, J. Rigby, C. Oprea, T. Troczynski, G. Oprea, Hydration studies on magnesia-containing refractories, in: Proceedings of UNITECR' 2003, 2003, pp. 51–63.
[25] M.D.M. Innocentini, M.G. Silva, B.A. Menegazzo, V.C. Pandolfelli, Permeability of refractory castables at high temperatures, J. Am. Ceram. Soc. 84 (3) (2001) 645–647.
[26] M.D.M. Innocentini, C. Ribeiro, R. Salomão, L.R.M. Bittencourt, V.C. Pandolfelli, Assessment of mass loss and permeability changes during the dewatering process of refractory castables containing polypropylene fibers, J. Am. Ceram. Soc. 85 (8) (2002) 2110–2112.
[27] M.D.M. Innocentini, A.R. Studart, M.M. Akyioshi, A.E.M. Paiva, L.R.M. Bittencourt, V.C. Pandolfelli, The drying behavior of high-alumina ultra-low cement refractory castables under different heating rates, Refract. Appl. News 7 (5) (2002) 17–20.
[28] M.D.M. Innocentini, F.A. Cardoso, M.M. Akyioshi, V.C. Pandolfelli, Drying stages during the heating of high-alumina, ultra-low cement refractory castables, J. Am. Ceram. Soc. 86 (7) (2003) 1146–1148.
[29] M.D.M. Innocentini, M.F.S. Miranda, F.A. Cardoso, V.C. Pandolfelli, Vaporization processes and pressure buildup during dewatering of dense refractory castables, J. Am. Ceram. Soc. 86 (9) (2003) 1500–1503.
[30] R. Salomão, V.C. Pandolfelli, Drying behavior of polymeric fiber-containing refractory castables, J. Tech. Assoc. Refract. Japan 24 (2) (2004) 83–87.
[31] A.R. Studart, I.R. de Oliveira, M.D.M. Innocentini, V.C. Pandolfelli, Effect of dispersant and fine powders on aluminum containing refractory castables, Am. Ceram. Soc. Bull. 84 (9) (2004) 9101–10107.
[32] S. Chartterji, Mechanism of expansion of concrete due to the presence of dead-burnt CaO and MgO, Cem. Concr. Res. 25 (1) (1995) 51–56.
[33] W.H. Gitzen, L.D. Hart, Explosive spalling of refractory castables bonded with calcium aluminate cement, Am. Ceram. Soc. Bull. 40 (8) (1961) 503–507.
[34] F.A. Cardoso, M.D.M. Innocentini, M.M. Akiyoshi, V.C. Pandolfelli, Effect of curing conditions on the properties of ultr-low cement refractory castables, Refract. Appl. News 9 (2) (2004) 12–16.
[35] F.A. Cardoso, M.D.M. Innocentini, M.M. Akiyoshi, V.C. Pandolfelli, Effect of curing time on the properties of CAC bonded refractory castables, J. Eur. Ceram. Soc. 24 (7) (2004) 2073–2078.